

A NUMERIC STUDY OF POWER EXPANSIONS AROUND SINGULAR POINTS OF ALGEBRAIC FUNCTIONS, THEIR RADII OF CONVERGENCE, AND ACCURACY PROFILES

DOMINIC C. MILIOTO

ABSTRACT. An efficient method of computing power expansions of algebraic functions is the method of Kung and Traub [4] and is based on exact arithmetic. This paper shows a numeric approach is both feasible and accurate while also introducing a performance improvement to Kung and Traub's method based on the ramification extent of the expansions. A new method is then described for computing radii of convergence using a series comparison test. Series accuracies are then fitted to a simple log-linear function in their domain of convergence and found to have low variance. Algebraic functions up to degree 50 were analyzed and timed. A consequence of this work provided a simple method of computing the Riemann surface genus and was used as a cycle check-sum. Mathematica ver. 13.2 was used to acquire and analyze the data on a 4.0 GHz quad-core desktop computer.

1. INTRODUCTION

The objective of this paper is five-fold:

- (1) Provide a simple method of analyzing the branching geometry of algebraic functions,
- (2) Describe a new method of determining radii of convergence,
- (3) Construct accuracy and order functions of series expansions around singular points,
- (4) Analyze test cases and summarize convergence, accuracy, and timing results,
- (5) Provide an accessible teaching aid of this subject to interested readers.

The functions studied in this paper are algebraic functions $w(z)$ defined implicitly by the irreducible n -degree expression in w :

$$f(z, w) = a_0(z) + a_1(z)w + a_2(z)w^2 + \cdots + a_n(z)w^n = 0 \quad (1)$$

with z and w complex variables and the coefficients, $a_i(z)$, polynomials in z with rational coefficients. By the Implicit Function Theorem, (1) defines locally, an analytic function $w(z)$ when $\frac{\partial f}{\partial w} \neq 0$. The solution set of (1) defines an algebraic curve, $w(z)$, and it is known from the general theory of algebraic functions that $w(z)$ can be described in a disk centered at z_0 by n fractional power series called Puiseux series with radii of convergence extending at least to the distance to the nearest singular point. In an earlier paper by this author [7], the method of Kaub and Traub was used to compute the power expansions, and a numeric integration method was described to compute their radii of convergence. In this paper, a new method to compute radii of convergence is described, and the accuracy of the series is studied in their domain of convergence.

A Puiseux expansion of (1) at a point z_0 is a set of n fractional power expansion in z given by

$$\{P_i(z)\} = \{w_i(z)\} = \sum_{k=r}^{\infty} a_k(z - z_0)^{\frac{m_k}{c}}, \quad i = 1, 2, \dots, n \quad (2)$$

Date: September 7, 2023.

2010 Mathematics Subject Classification. Primary 14O1; Secondary 14O4.

Key words and phrases. Puiseux series, fractional power series, algebraic functions, radius of convergence, Newton-polygon.

where z lies in the domain of convergence of the series. For finite z_0 , f is translated via $f(z + z_0, w)$ then $w(z)$ expanded as the set $\{w_i(z)\} = \sum_{k=r}^{\infty} a_k z^{\frac{m_k}{c}}$ with $z^{\frac{m_k}{c}}$ interpreted as principal-valued, and the series evaluated at the relative coordinate $z_r = z - z_0$.

In the case of an expansion at infinity, f is translated via $g(z, w) = z^\delta f\left(\frac{1}{z}, w\right)$ where δ is the largest exponent of z in $f(z, w)$. Then an expansion of $w(z)$ at the origin in terms of $g(z, w)$ is an expansion of $w(z)$ at infinity with the series evaluated at $z_r = \frac{1}{z}$. Section 14.4 is an example of an expansion at infinity. The derivative of $w(z)$ at a point $(z, w) = (p, q)$ can be computed as

$$\frac{dw}{dz} = \lim_{(z,w) \rightarrow (p,q)} \left(-\frac{f_z(z, w)}{f_w(z, w)} \right) \quad (3)$$

when this limit exist. A singularity $\{z_s, w_s\}$ of $w(z)$ is a point where the limit does not exist and in this paper, the term “singular point” refers to the z -component of the singularity.

2. CONVENTIONS USED IN THIS PAPER

- (1) Computations are computed with a working precision of 1000 digits. An exception to this are the accuracy and order functions which do not need this level of precision and are only computed to machine precision. All reported data however are shown with six or fewer digits for brevity.
- (2) Accuracy is the number of accurate digits to the right of a decimal point. Precision is the total number of accurate digits in a number. For a number x , $p = a + \log_{10} |x|$ with p the precision and a the accuracy.
- (3) Finite singular points are the zeros of the resultant of f with $\frac{\partial f}{\partial w}$ and are arranged into three lists:
 - (a) **The singular list:** This is a list of the finite singular points in order of increasing distance from the origin. Conjugate singular points are ordered real part first then imaginary part. The singular points are labeled s_1 through s_T with T the total number in the list,
 - (b) **The singular sequence:** For each singular point s_b , the remaining singular points are ordered in increasing distance from s_b ,
 - (c) **The comparison sequence:** This is a truncated singular sequence which is used to identify convergence-limiting singular points (CLSPs).
- (4) Each singular point is assigned a circular perimeter with radius equal to 1/3 the distance to the nearest singular point. This circle is called the singular perimeter.
- (5) A k -cycled branch refers to a part of $w(z)$, k -valued and represented by k Puiseux series with radius of convergence R .
- (6) The expansions of (1) at a singular point s_b is a set of n Puiseux expansions, $\{P_i(z)\}$ in terms of $z^{1/c}$ where c is a positive integer and can be different for different series in the set. c is both the cycle size of the series and cycle size of the branch represented by the series. For example, the power series $\sum_{k=r}^{\infty} a_k z^{\frac{m_k}{3}}$ has a cycle size of 3 and represents a 3-cycle branch: The branch has three coverings over a deleted neighborhood of the expansion center and is represented by three such Puiseux expansions making a 3-cycle conjugate set of power expansions. The geometry of the branch is similar to the geometry of $z^{\pm 1/3}$.

The set of n expansions are numbered 1 through n with conjugate members sequentially numbered. For example, a 15-degree function may have a 5-cycle branch with series numbers $\{7, 8, 9, 10, 11\}$, a 1-cycle branch with series number $\{12\}$, a 3-cycle branch with members $\{13, 14, 15\}$, and a 6-cycle with members $\{1, 2, 3, 4, 5, 6\}$.

(7) Branches of algebraic functions are categorized according to their algebraic and geometric morphologies into six types: $T, E, F_p^q, V_p^q, P_p^q, L^q$. The T, E and L^q branches are 1-cycle branches, and F_p^q, V_p^q and P_p^q are p -cycle branches. Appendix 16 describes each branch type.

(8) Reference is made to a base singular point s_b . This refers to a center of expansion of a Puiseux series with s_b a singular point. In the procedure described below, the branch surfaces about s_b are analytically continued over other singular points s_n in order of increasing distance from the base singular point until the nearest convergence-limiting singular point (CLSP) is encountered.

Another closely related term is the impinging singular point or ISP of a branch sheet. The ISP of a single-valued sheet of a multivalued branch is the nearest singular point impeding the analytic continuity of the branch surface. The nearest ISP of all branch sheets in a conjugate set is the CLSP for the branch and establishes the radius of convergence of their power expansions.

The CLSP of a conjugate set is not unique as multiple (conjugate) singular points may impinge the analytic continuity of a branch sheet. In these cases, the first member in the singular sequence is selected as the CLSP.

(9) R is a positive real number representing the radius of convergence of a power series centered at a singular point s_b . The value of R is expressed in terms of the associated CLSP. For example, if a power expansion has a center at the tenth singular point s_{10} , and its CLSP was found to be s_{25} , then $R = |s_{10} - s_{25}|$. This notation is presented as the exact symbolic expression for radius of convergence.

(10) The Puiseux expansions of $w(z)$ at a point s_b are grouped into conjugate classes. For example, a 5-cycle branch of $w(z)$ is expanded into five Puiseux series in powers of $z^{1/5}$, one series for each single-valued sheet of the branch. These five series make up a single 5-cycle conjugate class. The sum of the conjugate classes at a point z is always equal to the degree of the function in w . A power expansion of a 10-degree function consist of the set $\{P_i\}$ such that the sum of the conjugate types is 10. This could consists of a single 10-cycle conjugate class containing ten series, or three different 3-cycle conjugate classes and a single 1-cycle conjugate class or some other combination of conjugate classes adding up to 10. One member of each conjugate class is selected as the class generator. Each series member in a conjugate class can be generated by conjugation of a member of the class as follows:

Let

$$P_k(z) = \sum_{i=r}^{\infty} a_i z^{\frac{m_i}{c}} \quad (4)$$

be the k -th member of a c -cycle conjugate class of Puiseux series where all $\frac{m_i}{c}$ exponents are placed under a least common denominator c and $z^{\frac{m_i}{c}}$ is the principal-valued root. Then the c members of this conjugate class are generated via conjugation of (4) as follows:

$$P_j(z) = \sum_{k=r}^{\infty} a_k \left(e^{\frac{2j\pi i}{c}} \right)^{m_k} z^{\frac{m_k}{c}}; \quad j = 0, 1, \dots, c-1. \quad (5)$$

(11) The order of a n -cycle series of length l is denoted by \mathcal{O} and is the highest integer power of z in the series nearest to the exponent of the l 'th term. Accuracy measurement in this study are done

relative to a series order and not to a specific number of series terms and therefore accuracy results of multiple series will often include series of different lengths. For example, 500 terms of a 1-cycle series can have an order of 500 whereas 500 terms of a 20-cycle series may only attain an order of 30 if the expansion has many fractional exponents in the series.

- (12) If an expansion of an n -degree function produces n series in terms of $z^{1/n}$, the function fully-ramifies into a single n -cycle branch producing n series belonging to an n -cycle conjugate class. The branch is morphologically similar to $z^{\pm 1/n}$. An n -degree function minimally-ramifies at a singular point if it ramifies into a single 2-cycle branch and $(n - 2)$ single-cycle branches.
- (13) Absolute coordinates and relative coordinates in the z -plane are used. An absolute point z_a is a point in the z -plane. A relative point z_r is a point relative to a finite singular point s_b given by

$$z_a = s_b + z_r, \quad (6)$$

and in the case of an expansion at infinity,

$$z_a = \frac{1}{z_r}.$$

This is necessary for the following reasons:

- (a) Power series are generated relative to an expansion center, s_b . For example if the expansion center is $s_b = 1 + i$ and the series is evaluated at $z_r = 0.25$, the accuracy is determined by computing a higher precision branch value v_b by first solving for the roots $\{w_i\}$ of $f(1.25 + i, w) = 0$ and identifying which root v_b corresponds to the series value at z_r .
 - (b) The point D in Figure 3 is an absolute point. If $s_b = 2 + 2i$ and $D = 1.7 - 1.8i$, in order to evaluate a series expansions at D , the absolute point $D = 1.7 - 1.8i$ is first converted to the relative point $z_r = 1.7 - 1.8i - (2 + 2i) = -0.3 - 3.8i$.
 - (c) A series is evaluated over a list of points $C = \{z_i\}$ on a circle around the singular point s_b to compute accuracy profiles. The points $C = \{z_i\}$ are relative coordinates to s_b . The points in C are translated to absolute coordinates as $C_a = \{s_b + z_i\}$, then the roots $\{w_i\}$ of $f(w, C_a) = 0$ are computed to a higher precision and corresponding branch values identified to determine series accuracies.
 - (d) An expansion at infinity is generated relative to an expansion at zero, and the associated power expansions use relative coordinates $z_r = \frac{1}{z_a}$. See Section 14.4.
- (14) The series comparison test used to determine CLSPs relies on comparing a base series value v_s of a branch expansion at a point D in Figure 3 to a list of series values $\{u_i\}$ computed at the next nearest singular point s_n at point D . Since this involves comparing numeric values at finite precision, a separation tolerance s_t is used to identify a match. s_t is 1/10'th the minimum separation of the members in $\{u_i\}$. If $|v_s - u_k| < s_t$, then the k 'th series value at s_n is a match for v_s . If this tolerance is exceeded as in the case of branch values being very close to on another, or an insufficient number of terms in the series, or multiple matches, the series comparison test halts and the analysis reverts to the numerical integration method. This is described further in Section 10.2
- (15) An accuracy profile of a conjugate set of series is generated by computing the accuracy of generator series over a region in their domain of convergence. For each value $|z| < R$, the accuracy is determined by comparing the series results to more precise roots $\{w_i\}$ of $f(z, w) = 0$. These roots are computed with Mathematica's `NSolve` function. This accuracy is then fitted to an accuracy function $A(r_f, o)$.

(16) Table 1 is a list of symbols used in this paper.

TABLE 1. Symbols

Symbol	Description
m	Number of series terms used in a calculation
M	Maximum number of terms in a series
R	Radius of convergence
r_f	A positive rational number between 0 and 1
r	Radius of $z = re^{it}$
s_a	Series accuracy
$A(r_f, o)$	Accuracy function. (Section 12)
e_a	Expected accuracy at $ z < R$ given by $A(r_f, o)$
$\mathcal{O}(r_f, e_a)$	Order function (Section 11)
(a, b, c, d)	Coefficients of accuracy profile function
s_b	Singular point at center of expansion
s_n	Singular point n in the singular list
z_a	Absolute coordinate value of z
z_r	Relative coordinate of z_a with respect to a singular point
$\{w_i\}$	n values of $w(z_a)$ computed to high precision
$\{v_b\}$	Particular set of branch values with $\{v_b\} \subseteq \{w_i\}$
$\{v_s\}$	Branch series values at z_r corresponding to the set $\{v_b\}$
c_e	Comparison error given by $c_e = w_i - v_s $
r_t	Residual tolerance. (Section 5)
s_t	Separation tolerance. (Section 10.2)
m_s	Minimum separation. (Section 10.2)
s_f	Separation factor. (Section 10.2)
c_z	Coefficient zero. (Section 3)
$\{c_i\}$	Roots to the polygonal characteristic equation
N_{zm}	Maximum number of zero modular terms. (Section 6)
\mathcal{G}	Riemann surface genus. (Section 13)
\mathcal{K}	Riemann-Hurwitz sum (Section 13)

For example, let $z = r_f Re^{it}$ with R the radius of convergence of a series. v_s is the value of the series at z . v_b is the value of the corresponding branch at z computed to a higher precision than the series precision. $c_e = |v_b - v_s|$ is the comparison error. The accuracy of the series then becomes the negative of the exponent of c_e .

Generator series are evaluated in their domain of convergence along circular domains $|z| < R$ and the accuracy determined by comparing to the corresponding member in the set $\{w_i\}$. The accuracies are then fitted to an accuracy function $A(r_f, o)$ which gives the expected accuracy, e_a , of the series as a function of the radial ratio r_f and order o of the series. Solving for o in $e_a = A(r_f, o)$ gives $o = \mathcal{O}(r_f, e_a)$ which is the order function for estimating the order of a series needed for a desired accuracy e_a at $z = r_f Re^{it}$.

The genus, \mathcal{G} , of $w(z)$ is easily calculated via the Riemann-Hurwitz formula once conjugate classes at all singular points are found. The Riemann-Hurwitz sum \mathcal{K} must be an even number and serves as a necessary (but not sufficient) check-sum of the overall cycle geometry. See Section 13.

(17) Power expansions are generated by the Newton Polygon method [4]. This algorithm has two types of function iterations:

- (a) **Polygon iteration:** The first step in the algorithm is to create a Newton polygon establishing the initial terms of each expansion. If there are multiple roots in the resulting characteristic

equation, a new Newton polygon is created by iteration via the expression

$$f_2 = z^{-\beta_i} f(z, z^{\lambda_i}(w + c)) \quad (7)$$

and a second Newton polygon created for f_2 . If the resulting characteristic equation has multiple roots, polygon iterate f_3 of f_2 created and so on until the characteristic roots are simple. The substitution $f(z, z^{\lambda_i}(w + c))$ can cause numerical errors if not pre-processed beforehand. See Section 3.

- (b) **Newton Iteration:** Upon obtaining simple characteristic roots, the final polygon iterate f_n , after two additional transformations, is iterated by a Newton-like iteration to produce the desired number of expansion terms via the expression

$$w_{j+1} = w_j - \text{mod} \left(\frac{\bar{f}(z, w_j)}{f_w(z, w_j)}, z^{2^{(j+1)}} \right); \quad w_0 = c_i. \quad (8)$$

In the case of fractional polynomial solutions, the modular function continues to return zero after reaching the polynomial. Finite polynomial solutions however have to be distinguished from infinite solutions with extremely large gaps in exponents between successive series terms which would also return zero for a (often small) number of iterations. This is done by setting the number of maximum modular zeros, N_{zm} to a large but manageable number. In this case, N_{zm} was set to 15.

See [Determining radii of convergence of fractional power expansions around singular points of algebraic functions](#) for additional information about these concepts.

This study is organized as follows:

- (1) Compute the singular points to 1000 digits of precision,
- (2) Compute conjugate classes at all singular points,
- (3) Compute at least 1000 terms of each branch expansion at a base singular point s_b with a working precision sufficient to obtain series with at least 900 digits of precision,
- (4) Compute expansions for all singular points in the comparison sequence to at least 100 terms,
- (5) Estimate radius of convergence for each branch around s_b using the Root Test,
- (6) Compute CLSPs via the comparison test and integration test,
- (7) Compute the accuracy function $A(r_f, o)$ and order function $O(r_f, e_a)$,
- (8) Generate convergence, accuracy, and timing data for six test functions.

3. PRECISION OF COMPUTATIONS

The precision of a series is limited by the precision of the singular points as well as the reduction in precision incurred by various steps in the Newton polygon procedure.

Figure 1 is a precision plot of the five generator series for Test Case 1 and exhibits a reduction in precision after each Newton iteration. For example, the 1-cycle T branch shown as the purple line begins with 1000 digits of precision dropping to 918 digits at the 1024'th term. The precision of each series is therefore dependent on the the number of terms used. If the $1T$ series was evaluated very close to its center of expansion, the accuracy could rapidly increase as additional terms are added to the computation. At some point, the precision of the results could approach the maximum precision of the series and no longer increase as more terms are used leading to a case in which the precision of the comparison error $c_e = |w_i - v_s|$ drops to zero. This would skew the accuracy results and subsequently the fit functions $A(r_f, o)$ and $O(r_f, e_a)$. To avoid this possibility, c_e values with zero precision are omitted from the accuracy results.

The Newton polygon algorithm produces translated functions $f(z + s_i, w)$ and $f(z, w + c_i)$. These substitutions can create coefficients which are actually zero but due to finite numerical precisions, result in very small residual values. Two residual conditions arise which are processed in the following order:

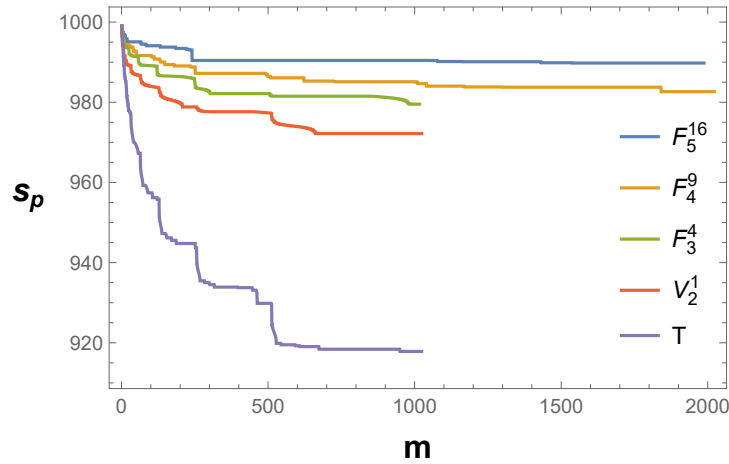


FIGURE 1. Precision Profile Plot

- (1) **R1:** A singular point can be a zero to a coefficient of the transformed function $f(z + s_i, w)$. These are called coefficient zeros denoted by the symbol c_z . Since the singular points are computed to a finite number of digits, coefficients which are actually zero can have very small non-zero residues. If not eliminated, this would cause incorrect polygon calculations. The two sets $\{p_i\}$ and $\{q_i\}$, described below, are such singular points. There may however exist other singular point zeros. $f(z, w)$ is pre-processed to remove these zero coefficient before the substitution $f(z + s_i, w)$.
- (2) **R2:** Roots $\{c_i\}$, of the polygonal characteristic equations are substituted into the polygonal iterates as $f(z, z^\lambda(w + c_i))$ and likewise results in zero coefficients which may have very small residues and must be removed. Similar to the **R1** pre-processing, these coefficients are first identified and removed prior to the substitution $w \rightarrow w + c_i$.

3.1. Additional precision issues.

- (1) Singular points with very small absolute values can lead to very small coefficients in the translated function $f(z + s_i, w)$ if the function has high powers of z . For example if $s_i = 1/1000$, then the substitution $z \rightarrow z + s_i$ into z^{50} leads to a coefficient on the order of 10^{-150} , and this small value must not be lost due to inadequate numerical precision as doing so would adversely affect the polygonal iteration step of the Newton polygon algorithm producing incorrect initial segments. Since the test cases below were run with an average precision of 1000, this particular cases would be correctly processed. However, there exists functions with arbitrarily small singular sizes which would be mis-handled. The singular size therefore is carefully monitored and if the size exceeds the precision limitation of the calculation, the procedure is halted.
- (2) **Multiple polygon iteration** Each polygon iterates of (7) can reduce the precision of the resulting function iterate f_i .
- (3) **Limitations of Mathematica's NSolve function:** Roots returned by NSolve are limited in precision to the precision of the input equations. If the equations are at 1000 digits of precision, then the maximum precision of the roots is 1000. However, the precision of the roots returned by NSolve may be less than the precision of the equations. For example, the roots of $1/2 + x^2$ returned by NSolve when the precision of the equation is set to 1000 is 1000. However, if the precision of $1/4 + x + x^2$ is set to 1000, NSolve returns roots to only 500 digits of precision.

4. COMPUTING THE SINGULAR POINTS

The finite singular points are computed by solving for the zeros of the resultant of f with $\frac{\partial f}{\partial w}$ using Mathematica's NSolve function. This computation is CPU-intensive when f is of high degree and the coefficients $c_i(z)$ are non-sparse and high degree. The 50-degree function studied in Test Case 4 took 3.8 hours to compute 4584 singular points to 1000 digits of precision, whereas a random 20-degree function with 156 singular points and low degree coefficients takes about one second.

There are two sets of singular points by inspection:

- (1) Roots of $a_0(z)$ if $a_1(z) = 0$: These are the set $\{q_i\}$,
- (2) Roots of $a_n(z)$: These are the set of poles $\{p_i\}$.

5. COMPUTING INITIAL TERMS AND IDENTIFYING CONJUGATE CLASS MEMBERSHIP

The method of Kung and Traub [4] implements Newton polygons to generate the initial terms (segments) of each power expansion. See also [7] for more information about Newton polygons. For a generic polynomial, computing the initial terms requires only a few iterations of Newton polygon and is executed quickly. Even the 50-degree polynomial in Test Case 5, required at most two seconds to compute the initial segments at a singular point.

However, in many cases, not all initial segments require further expanding. Rather, in this paper the initial terms are first used to identify the cycle size of each expansion and their conjugate class membership. Class membership is obvious from the initial segment exponents when there are distinct multi-cycles. In the case of multiple k -cycle segments, membership is determined by conjugating the initial terms in order to determine which expansions belong to each conjugate set. One member of each class is selected as the class generator and further expanded via Kung and Traub's method of iteration.

Consider an expansion at the origin of the following 12-degree function:

$$f(z, w) = w^4 z (a_2 (1 - w^2 (a_2^*)^2))^4 - (a_2^* (a_2^2 - w^2))^4; \quad a = 2/3 + i/4, \quad (9)$$

and the initial terms obtained from the Newton Polygon step given by (10). Since there are 12 expansions all of which are 4-cycle, there are three 4-cycle conjugate classes of branch expansions:

$$\begin{aligned} P_1(z) &= -0.667 - 0.25i - (0.28 + 0.244i)z^{1/4} \\ P_2(z) &= -0.667 - 0.25i - (0.244 - 0.28i)z^{1/4} \\ P_3(z) &= -0.667 - 0.25i + (0.244 - 0.28i)z^{1/4} \\ P_4(z) &= -0.667 - 0.25i + (0.28 + 0.244i)z^{1/4} \\ P_5(z) &= 0.667 + 0.25i - (0.28 + 0.244i)z^{1/4} \\ P_6(z) &= 0.667 + 0.25i - (0.244 - 0.28i)z^{1/4} \\ P_7(z) &= 0.667 + 0.25i + (0.244 - 0.28i)z^{1/4} \\ P_8(z) &= 0.667 + 0.25i + (0.28 + 0.244i)z^{1/4} \\ P_9(z) &= -\frac{1.973}{z^{1/4}} \\ P_{10}(z) &= -\frac{1.973i}{z^{1/4}} \\ P_{11}(z) &= \frac{1.973i}{z^{1/4}} \\ P_{12}(z) &= \frac{1.973}{z^{1/4}}. \end{aligned} \quad (10)$$

In order to determine which expansions belong to each 4-cycle conjugate class, segment members are conjugated. Consider:

$$P_1(z) = (-0.666667 - 0.25I) - (0.2799 + 0.244276I)z^{1/4}.$$

Conjugation of P_1 produces the following list of members:

$$\begin{aligned}
 & (-0.666667 - 0.25i) - (0.2799 + 0.244276i)z^{1/4} \\
 & (-0.666667 - 0.25i) + (0.244276 - 0.2799I)z^{1/4} \\
 & (-0.666667 - 0.25i) + (0.2799 + 0.244276I)z^{1/4} \\
 & (-0.666667 - 0.25i) - (0.244276 - 0.2799I)z^{1/4},
 \end{aligned} \tag{11}$$

and these are P_1 through P_4 . Therefore, P_1 through P_4 are the four members of a 4-cycle conjugate class $1V_4^1$ and the series numbers for this set are $\{1, 2, 3, 4\}$. Conjugating expression $P_5(z)$ in 10 gives the next four series, $\{5, 6, 7, 8\}$ making up a second 4-cycle class $2V_4^1$, and conjugating P_9 gives the set of the next four series, $\{9, 10, 11, 12\}$ making up a third 4-cycle conjugate set $3P_4^{-1}$. Series 1, 5, and 9 are selected as the generators of the three conjugate classes and further expanded via Newton Iteration. Once the desired number of terms for each generator series has been computed, the full 12 expansions around this singular point can be generated by conjugating the generator series. Since conjugation is much faster than Newton iteration, computing the 12 series this way is faster than generating each member separately via Newton Iteration.

Computing 1024 terms of each generator series at 1000 digits of precision took 3.4 minutes. Conjugation of all generators took one second. Compared to expanding all initial segments, this represents a four-fold reduction in execution time. The performance gain is dependent upon the ramification extent at the expansion center with minimal gain obtained with minimal ramification.

6. EXPANDING THE INITIAL SEGMENTS VIA NEWTON-LIKE ITERATION

The following is a brief summary of the Kung and Traub method of iterating the initial series segments. For more information, interested readers are referred to the author's website: [Examples of power expansions around singular points of algebraic functions](#), which includes worked examples.

Consider the following function from the website:

$$f(z, w) = (z + z^2) + (1 + z)w + w^2 = 0. \tag{12}$$

Processing this function through the Newton Polygons twice produces the first two terms (initial segments) of each series

$$\begin{aligned}
 P_1(z) &= -2/3 - iz^{1/2} \\
 P_2(z) &= -2/3 + iz^{1/2},
 \end{aligned}$$

and the second function iterate $f_2(z, w)$.

A critical part of a numerical Newton polygon algorithm is accurately identifying multiple roots of the characteristics equation. This is accomplished by first setting the roots to the same precision. When two numbers accurate to a set precision are subtracted in Mathematica, the precision of the difference is zero. Thus, the roots are first set to the minimum precision of the set, and the differences between roots are checked with those having zero precision identified as multiples. Although the roots are computed with a default precision of 1000 digits, the actual precision can be significantly lower as described above. In these cases, the singular points are generated with a sufficient precision to obtain roots near 1000 digits of precision.

As the Newton polygon algorithm will often lead to fractional polynomials, f_2 is transformed into a polynomial with integer powers by the following two transformations:

$$\begin{aligned}\widehat{f}(z, w) &= \frac{1}{z^{\beta_k}} f_k(z, z^{\lambda_k} w) \\ \overline{f}(z, w) &= \widehat{f}(z^d, w)\end{aligned}\tag{13}$$

where k is the index of the last polygonal function which did not produce a characteristic equation with multiple roots (k is 2 in this case). Let d be the lowest common denominator of the exponents $\{\lambda_j\}$ for $j = 1, 2, \dots, k$ for each of the segments above. In this case, $k = 2$ and $d = 2$ with $\lambda_2 = 1/2$ and $\beta_2 = 1$. Therefore we have:

$$\begin{aligned}\widehat{f}(z, w) &= \frac{1}{z^{\beta_k}} f_k(z, z^{\lambda_k} w) \\ &= z^{-1} [(z + z^2) + z(z^{1/2}w) + zw^2] \\ &= 1 + z + z^{1/2}w + w^2 = 0\end{aligned}\tag{14}$$

and

$$\begin{aligned}\overline{f}(z, w) &= \widehat{f}(z^d, w) \\ &= 1 + z^2 + zw + w^2.\end{aligned}$$

In order to generate more terms of the series, Kung and Traub implements a Newton-like iteration on \overline{f} :

$$w_{j+1} = w_j - \text{mod} \left(\frac{\overline{f}(z, w_j)}{\overline{f}_w(z, w_j)}, z^{2^{(j+1)}} \right); \quad w_0 = \{i, -i\}\tag{15}$$

where the mod function extracts all terms of the Taylor expansion of the quotient with power less than $2^{(j+1)}$. Listing 1 is the modulus step in (15) implemented in Mathematica.

LISTING 1. Mathematica code

```
newtonIterate =  
  Normal[Series[fBar/fBarDeriv, {z, 0, 2^(j + 1) - 1}]];
```

Solutions with fractional polynomial solutions return sequential zero modular result after a finite number of iterations. In this study, this number of maximum zero modular values is N_{zm} and set to 15. See Test Case 14.2 for an example of a polynomial solution.

7. APPROXIMATING RADII OF CONVERGENCE VIA THE ROOT TEST

The Root Test is used to approximate the radius of convergence of a branch expansion in order to estimate the number of additional power expansions needed to identify the CLSP of the branch series. The Root Test however is not applicable to polynomial solutions which have infinite radii of convergence.

The standard definition is modified to include the branch cycle size:

$$R = \frac{1}{\liminf_{k \rightarrow \infty} |a_k|^{\frac{c}{m_k}}}\tag{16}$$

where c is the cycle size of the series, and the set $\{m_i\}$ is the set of exponent numerators under a least common denominator. For example, the terms $a_0 + a_1z + a_2z^{3/2} + a_3z^{9/4} + z^3$ would have the set $\{m_i\} =$

$\{0, 4, 6, 9, 12\}$. Then the radius of convergence of each branch expansion can be approximated by forming the set:

$$S = \left\{ \left(\frac{1}{m_k}, \frac{1}{|a_k|^{\frac{c}{m_k}}} \right) \right\}$$

and extrapolating $\lim_{k \rightarrow \infty} S$ using a sufficient number of trailing points of S . For example, consider 512 terms of a 2-cycle series:

$$a_1 z^{1/2} + a_2 z^2 + a_3 z^{5/2} + a_4 z^3 + \cdots + a_{512} z^{512}.$$

Therefore

$$S = \left\{ \left(\frac{1}{1}, \frac{1}{|a_1|^{1/2}} \right), \left(\frac{1}{4}, \frac{1}{|a_2|^{1/2}} \right), \left(\frac{1}{5}, \frac{1}{|a_3|^{2/5}} \right), \left(\frac{1}{6}, \frac{1}{|a_3|^{1/3}} \right), \cdots, \left(\frac{1}{1024}, \frac{1}{|a_{512}|^{1/512}} \right) \right\}.$$

The radius of convergence, R , is approximated by minimizing a suitable curve to the greatest lower bound of S using Mathematica's **Minimize** function and then extrapolating to zero. Linear, quadratic and cubic curves were used as test fit functions with the smallest residual error selected as the best fit. Figure 2 shows the generator series points for the F_5^{16} branch of Test Case 1 as blue points. The dashed red curve is the best fit of the greatest lower bound of points. The black point is the extrapolated value of 0.645 for the radius of convergence. The actual radius of convergence for this branch is $|s_{27}| \approx 0.641$. The CLSP for the power expansion are approximated by selecting a singular point with absolute value closest to the extrapolated point and then used to estimate the minimum number of singular points in the comparison sequence.

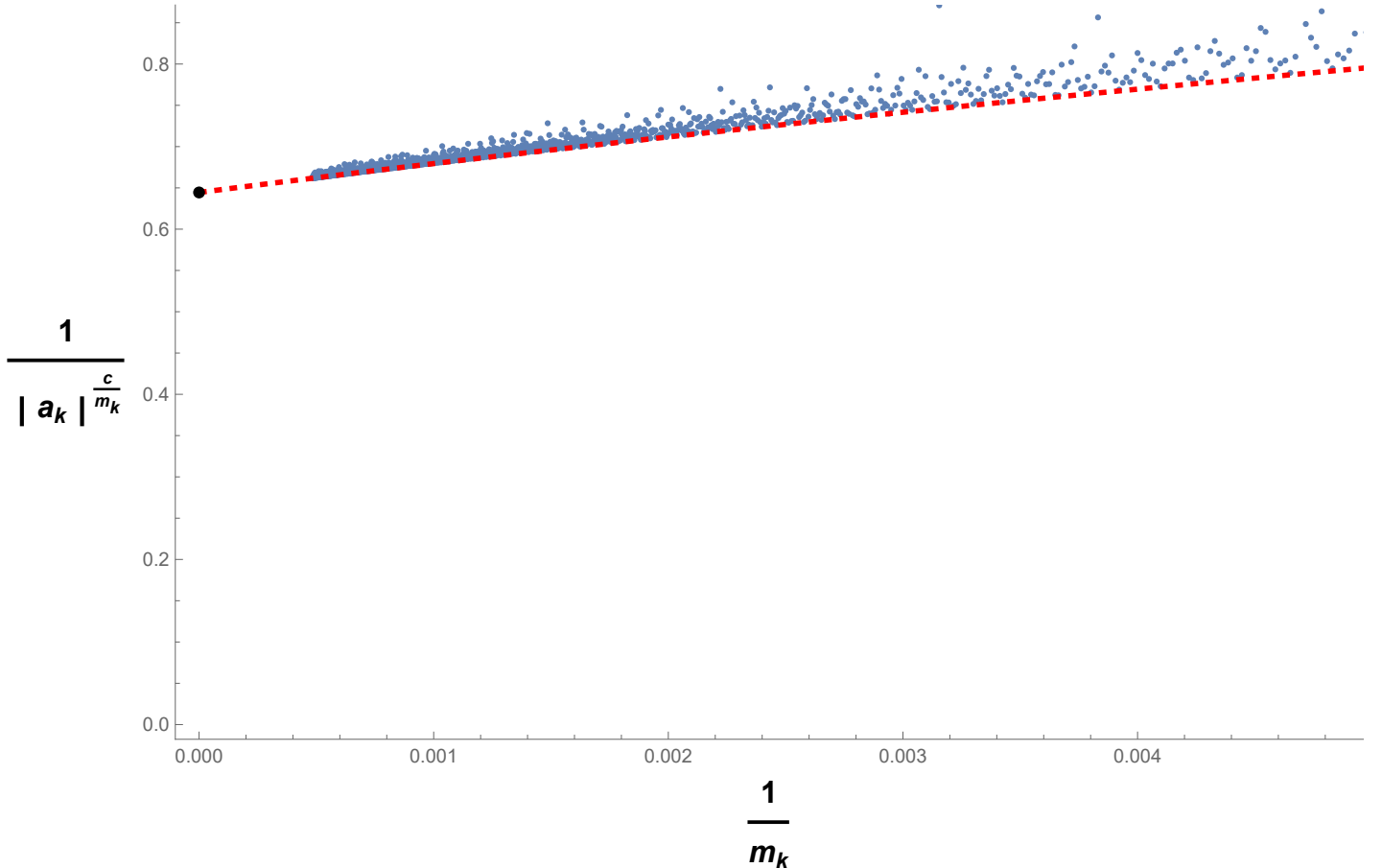


FIGURE 2. Root Test results of F_5^{16} branch of Test Case 1

8. COMPUTING THE COMPARISON SEQUENCE

The most distant estimated CLSP determined by the Root Test determines the minimum length of the comparison sequence used by the series comparison and integration tests to identify CLSPs at a base singular point s_b . Table 2 gives the Root Test results for Test Case 1, and since the expansion center is the origin, s_{118} is the most distant estimated CLSP giving a minimum comparison sequence s_2 through s_{118} .

Expansions must be generated at all singular points in the comparison sequence but do not require a large number of terms since these series are evaluated at their singular perimeter with good convergence. Since the Root Test is only an approximation for the most distant CLSP, a reasonable comparison sequence in this case is s_2 through s_{125} .

TABLE 2. Test Case 1 Root Test results at the origin

Index	Sheet	Type	Cycle Size	est. R	est. CLSP	Series size
1	1	F_5^{16}	5	0.64571	31	1987
2	6	F_4^9	4	0.50751	7	2022
3	10	F_3^4	3	0.16797	2	1017
4	13	V_2^1	2	0.16772	2	1024
5	15	T	1	1.0966	118	1024

9. COMPUTATION OF CONVERGENCE-LIMITING SINGULAR POINTS

9.1. Necessary and sufficient conditions for analytically-continuing a branch across a singular point:

- (1) In order to analytically continue a k -cycle branch from one singular point to the next nearest singular point, the next singular point must have at least k single-cycle analytic branches to support continuity, i.e., 1-cycle branches which do not have poles,
- (2) A k -cycle branch is continuous across a singular point if all branch sheets continue onto analytic 1-cycle branches,

Individual single-valued branch sheets of an k -cycle branch may continue across different singular points but the analytic region of the branch as well as the convergence domain of its power expansion is established upon analytic continuity with the nearest multi-cycle branch sheet or branch sheet with a pole. The first singular point in which this occurs is the CLSP for the associated set of conjugate Puiseux series and establishes their radii of convergence.

10. METHODS TO COMPUTE CLSPs

Two methods are used to find CLSPs:

10.1. Constructing an analytically-continuous route between singular points by numerical integration. Since the Puiseux series for (1) converge at least up to the next nearest singular point, an analytically-continuous route can be created between the perimeter of the base singular point and perimeter of the next nearest singular point. This is shown in Figure 3. In the diagram the circles are the singular perimeters. A straight line path between point A and D is given by the expression

$$z(t) = A(1 - t) + Dt; \quad 0 \leq t \leq 1, \quad (17)$$

and then each branch sheet of s_b is numerically integrated over the path from point A to point D onto a branch sheet of s_n via the following set of initial value problems:

$$\frac{dw}{dt} = -\frac{f_z}{f_w} \frac{dz}{dt}, \quad w_i(0) = P_i(A - s_b); \quad i = 1, 2, \dots, n \quad (18)$$

with $z(t)$ defined by (17), $0 \leq t \leq 1$, and each $P_i(z)$ is a Puiseux series at s_b . Each s_b branch sheet is then checked for analytic continuity over s_n as per Section 9.1. See also [9] for further background about this technique.

After s_n has been checked and branch sheets have been found to be continuous, a path to the next sequential singular point is created and the previously-continued branches tested for further continuity. However there is the possibility of attempting to continue a branch sheet to another singular point when a removable singular point is in the path of integration. Numerical integration will fail over a removable singularity even though the function is analytic because Equation (2) is used for the derivative and at a removable singular point, this quotient is indeterminate. In this case, the integration path is split into paths β_1 , around half the perimeter of the removable singular point E , and over β_2 shown in the second diagram of Figure 3.

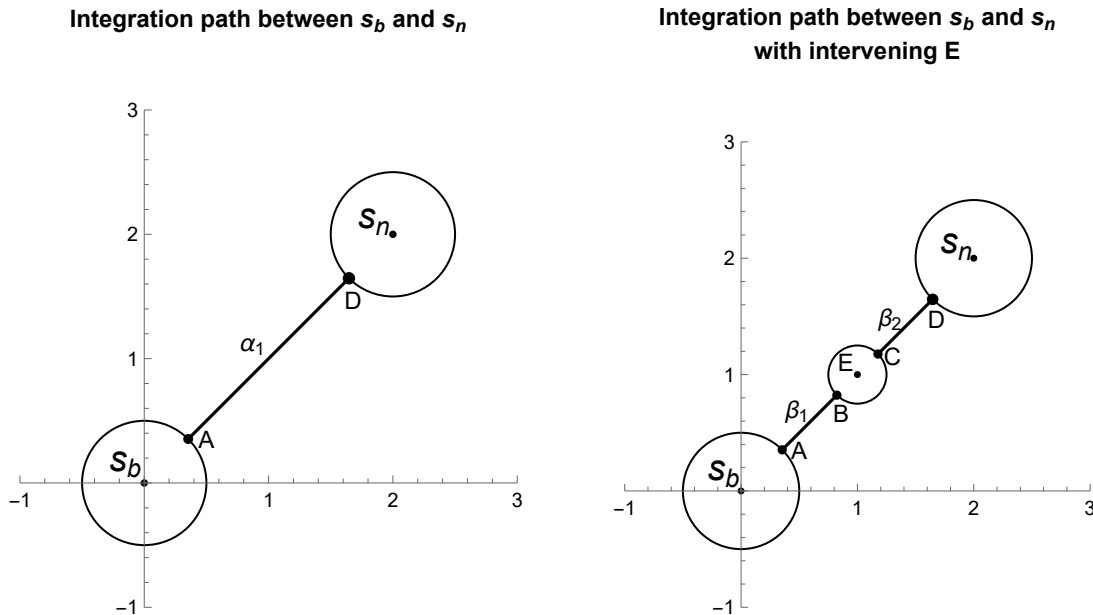


FIGURE 3. Continuation path used by numerical integration method

10.2. Identifying CLSPs by the series comparison test. This section introduces a simpler method for computing a CLSP based on a series comparison test.

In the series comparison test, the value of a base branch sheet at point D in Figure 3 is compared to the expansions centered at s_n at point D using the separation threshold s_t . Convergence of both series is guaranteed since the series centered at s_n converges on its perimeter, and convergence of the current analytically-continuous base series are guaranteed to converge at D since they converge at the previous $n - 1$ singular points. However, the convergence rate of the base sheets will decrease as successive singular points approach the CLSP of a base expansion sheet. This necessitates computing the base series at a sufficiently high precision and number of terms.

Using the data from Section 5, with three 4-cycle branches and three singular points, consider series 1 expansion at the origin with a value of $v_s = -0.92827 - 0.314806i$ at point D in Figure 3 and compare it with the 12 expansion values at s_2 at point D given in Table 3. In this case, there are no poles at s_1 and s_2 . The minimum distance between the points in Table 3 is 0.04 so that the separation threshold is $s_t = 0.04/10 = 0.004$ and clearly v_s is within this threshold for the third entry in this list. The actual difference between the two values in this test was 10^{-40} . Therefore, the branch sheet corresponding to series 1 continues onto the branch sheet associated with the third series at s_2 .

As the analysis moves farther away from the base expansion and nearer to the CLSP, the accuracy of the base expansions will decrease and may not satisfy the separation threshold or may produce multiple

TABLE 3. Branch sheet values at s_2

$-2.44964 - 1.22342i$
$-1.0006 + 1.0348i$
$-0.92827 - 0.314806i$
$-0.783318 + 0.21872i$
$-0.696357 - 0.639337i$
$-0.371485 - 0.178941i$
$0.371485 + 0.178941i$
$0.696357 + 0.639337i$
$0.783318 - 0.21872i$
$0.92827 + 0.314806i$
$1.0006 - 1.0348i$
$2.44964 + 1.22342i$

matches. This condition is checked in the algorithms and when encountered, the comparison test is halted and flagged for the numerical integration test.

11. ILLUSTRATIVE EXAMPLE OF RADIUS OF CONVERGENCE COMPUTATION USING SERIES COMPARISON TEST

Consider the function from Test Case 1:

$$f_1(z, w) = (z^{30} + z^{32}) + (z^{14} + z^{20})w^5 + (z^5 + z^9)w^9 + (z + z^3)w^{12} + (6)w^{14} + (2 + z^2)w^{15}. \quad (19)$$

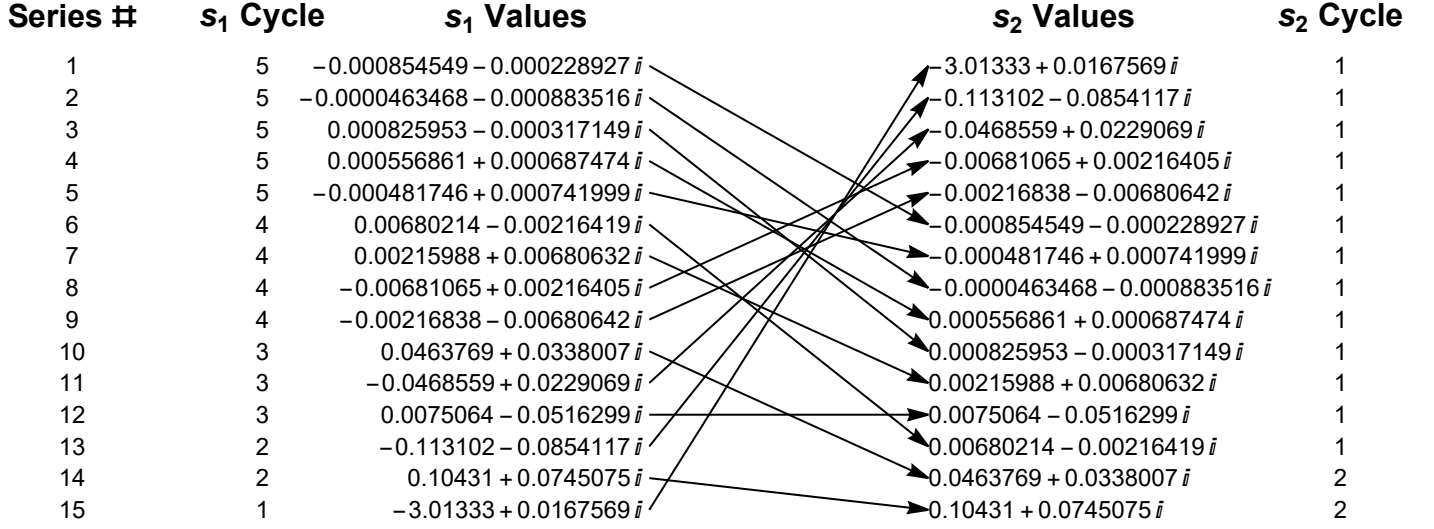
Figure 4 graphically illustrates the analytic continuation of all branch sheets at the expansion center s_1 , into the branch sheets of s_2 . For example, the first series at s_1 is a 5-cycle with the value at point D of $-0.000855 - 0.000229i$. Following the arrow from this point into the list of s_2 values, it continues onto sheet 6 of s_2 which is a 1-cycle. The remaining four sheets of this 5-cycle also continue onto 1-cycles of s_2 . Therefore, the 5-cycle at s_1 is analytically-continuous over s_2 .

Consider now series 10 of s_1 which is a 3-cycle branch. It continues onto series 14 of s_2 which is a 2-cycle branch. Therefore, the 3-cycle of s_1 is not analytically continuous over s_2 and so s_2 is the CLSP for this branch. Likewise the 2-cycle of series 14 of s_1 continues onto the second sheet of the 2-cycle of s_2 and therefore establishes the CLSP for this branch as well. Therefore the CLSP for the 3 and 2-cycle branches is s_2 . Next, analytic continuity of the 1, 4, and 5-cycle branches are checked over s_3 and if any are continuous, further singular points are checked in this way until all CLSPs are found.

12. CREATING ACCURACY PROFILE FUNCTIONS

Once the radii of convergence of a branch generator is determined, the accuracy of the series can be studied as a function of $|z| < R$ and series order \mathcal{O} . The accuracy of a series depends on four factors:

- (1) **Precision of series:** The precision of the series is limited to the precision of the expansion center, i.e., the singular points. For the test cases below, singular points were computed to about 1000 digits of precision. Also, the precision of the associated power expansions decrease after each iteration of the Newton iteration step as shown in Figure 1. For example, terms of the T series of Test Case 1 gradually drop to 918 digits of precision near the end of 1000 terms. This trend limits the maximum accuracy of a particular value of the series to the precision of the terms used.
- (2) **Number of terms:** The accuracy of an expansion was found to have a linear relation to the number of terms used in the expansion as illustrated in Figure 7.
- (3) **The absolute value of z relative to R :** The accuracy of an expansion exhibited a logarithmic dependence on $|z| < R$ as shown in Figure 6.

FIGURE 4. Test Case 1 analytic continuation between s_1 and s_2

(4) **Presence of nearby singular points.** The accuracy of a series at z is affected by the presence of nearby impinging singular points. This is further explained below.

An accuracy function $A(r_f, o)$ gives an expected accuracy of a series as a function of the radial ratio $0 < r_f < 1$ and order, o , of a series. An order function $O(r_f, e_a)$, for a given r_f and desired accuracy e_a , returns the estimated order of a series needed for the desired accuracy. The series is then be searched for the term m corresponding to this order, and terms 1 through m used to evaluate the accuracy of the series. Generator series are evaluated in their convergence domains and compared to more precise values of the function and fitted to accuracy functions. Letting the expected accuracy $e_a = A(r_f, o)$, and solving for o gives the order function.

However, the accuracy of a power expansion is not constant along a circle $z = r_f Re^{it}$ but varies slightly along the outermost region of convergence depending on the presence of impinging singular points. The F_5^{16} branch of Test Case 1 has conjugate series (1, 2, 3, 4, 5) with $R = s_{27} \approx 0.6413$. The impinging singular point of series 5 is s_{27} . Figure 5 is a plot of the log of the difference between the actual value of sheet 5 and 1987 terms of the series along a circle with $r_f = 15/26$, that is $r = 15/26R$. Notice how the difference is not constant around the circle but varies approaching a minimum accuracy at around an argument of 0.4. The red line in the plot is the argument of this branch sheet's ISP. Notice the peak matches this line at $\log(\Delta) = -238.59$. This and other cases suggest accuracy is affected by nearby impinging singular points. The ISPs accuracy effect is however small. Figure 5 reflects the log of the difference between the actual

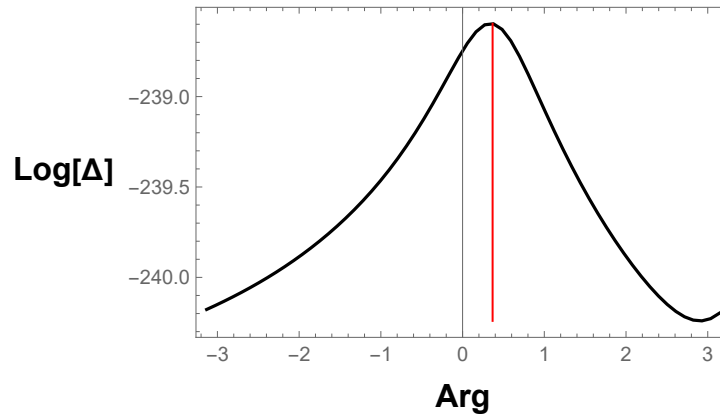


FIGURE 5. Minimum arc accuracy diagram

branch value and the series value which is more easily visualized. The actual minimum and maximum

difference is $(4.6 \times 10^{-105}, 2.39 \times 10^{-104})$. This study does not include this variation in accuracy, rather, random points along the circle $z = r_f Re^{it}$ are used as test points although including this effect would improve the accuracy of the fit functions.

Consider the accuracy results of 1287 terms of this branch for $1/25 \leq r_f \leq 24/25$. Results of this test are shown in Figure 6A and clearly shows a logarithmic trend. To this extent, the data points in Figure 6A are

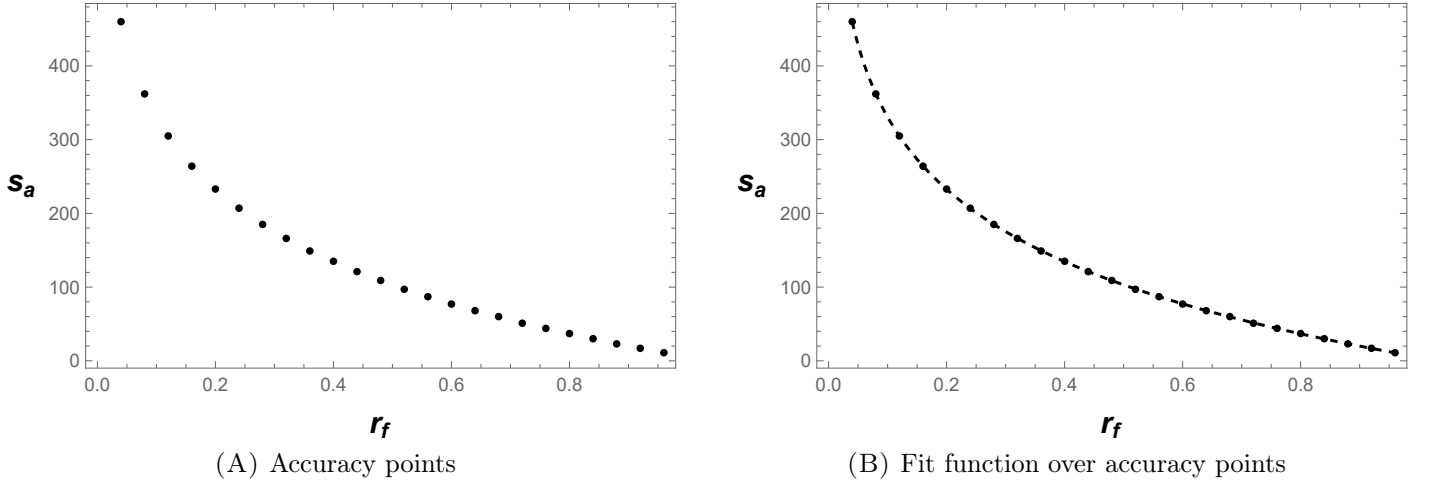


FIGURE 6. F_5^{16} accuracy profile as a function of r , 1549 terms

fitted to $L(r) = a + b \log(r)$. Figure 6B shows this fit as the dashed black line $L(r) = 3.3333 - 118.986 \log(x)$.

Consider next the accuracy trend at $r_f = 1/5$ for $20 \leq o \leq 400$ shown in Figure 7A. The accuracy data follows a linear trend and is fitted to $G(o) = 9.55371 + 0.0931429o$ in Figure 7B.

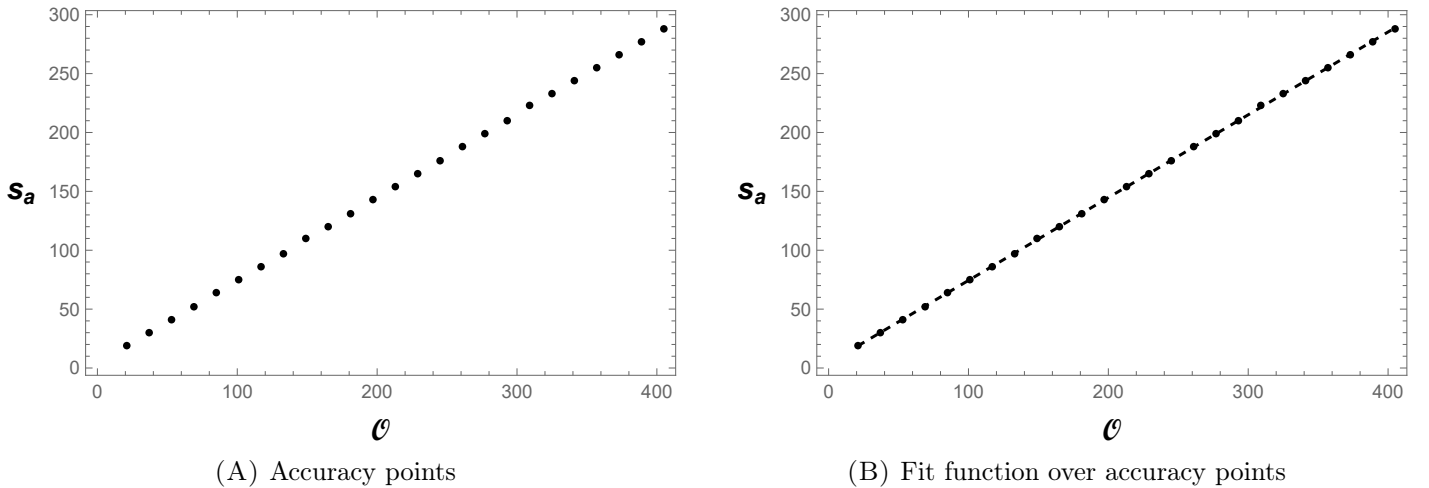


FIGURE 7. F_5^{16} accuracy profile as a function of order with $r_f = 1/5$

These accuracy trends are observed for all test cases studied in this paper.

When the accuracy data is plotted in space, the set of points shown in Figure 8A are obtained. Note in this figure the logarithmic trend over r_f and the linear trend over the series order o . So it is reasonable to construct a log-linear accuracy function given by

$$A(r_f, o) = a + b \log(r_f) + o(c + d \log(r_f)) \quad (20)$$

with r_f the radial ratio and o , the order of the series using Mathematica's `NonlinearModelFit` function. When this is done, the surface shown in 8B with $A(r_f, o) = 1.58647 - 6.67332 \log(r) + o(0.000684195 -$

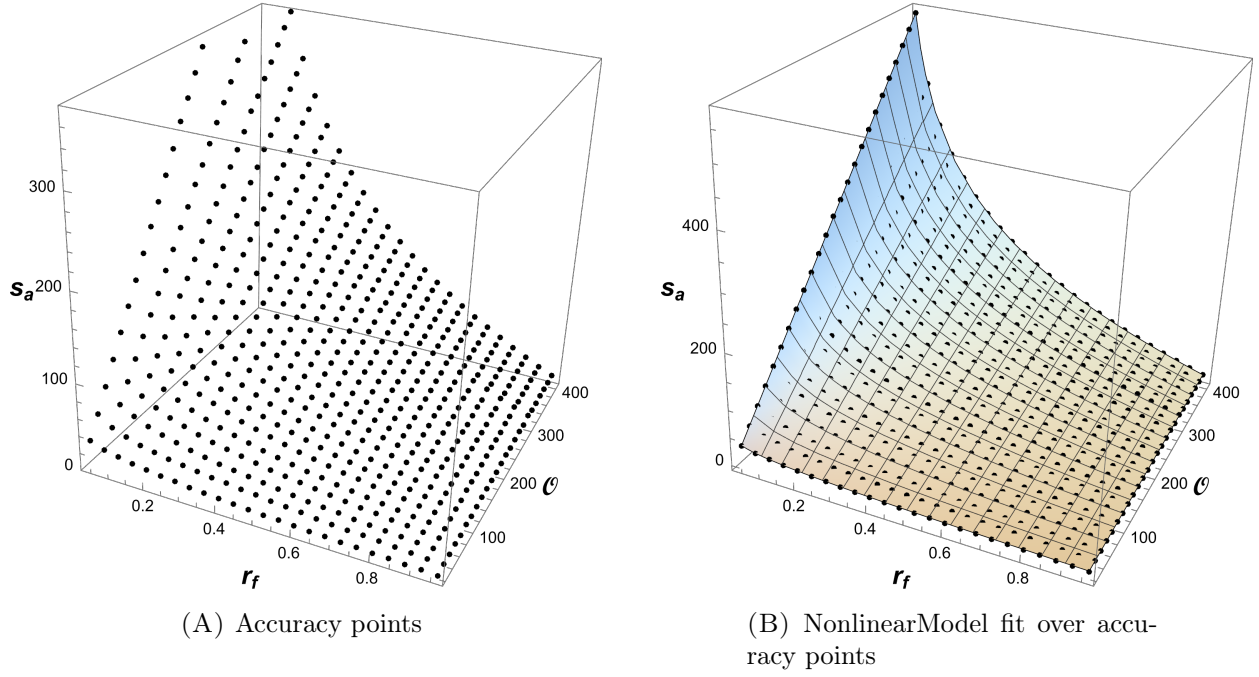


FIGURE 8. F_5^{16} accuracy profile as a function of r_f and \mathcal{O}

$0.0871573 \log(r))$ is generated which also shows the accuracy data as black points superimposed on the surface.

Letting $e_a = A(r_f, o)$ and solving for o gives the order function

$$O(r_f, e_a) = \left\lceil \frac{e_a - a - b \log(r_f)}{c + d \log(r_f)} \right\rceil \quad (21)$$

which estimates the order needed to achieve a particular accuracy e_a at r_f .

13. COMPUTING THE RIEMANN SURFACE GENUS USING THE RIEMANN-HURWITZ SUM

Once initial segments are computed for all singular points including the point at infinity, the Riemann surface genus is easily computed using the Riemann-Hurwitz formula in the form of

$$\begin{aligned} \mathcal{G} &= 1 + 1/2 \sum_S \sum_{i=1}^T (c_i - 1) - D \\ &= 1 + 1/2 \mathcal{K} - D \end{aligned} \quad (22)$$

where S is the set of singular points, and the double sum is over all conjugate groups of singular points with c_i the cycle size. D is the degree of the function in w . Note the Riemann-Hurwitz sum \mathcal{K} must be an even number and serves as a cycle check-sum: if it's odd a cycle error has occurred. However this is only a necessary condition for an error-free function ramification profile. As an example, Test Case 1 with 179 singular points has the ramification profile shown in Table 6. A total of 174 singular points each minimally ramify contributing a total of 174 to \mathcal{K} . s_1 contributes 10, s_{110} and s_{111} contribute 16 giving $\mathcal{K} = 200$. Then $\mathcal{G} = 200/2 + 1 - 15 = 86$. The time required for this calculation is predominantly the time to compute the singular points and initial segments.

14. TEST RESULTS

The following test cases include three data sets for each function:

- (1) Timing data to compute the singular points, segments, power expansions, and CLSPs,
- (2) Summary report of radii of convergence and accuracy results at a selected singular point,
- (3) Ramification profile summarizing the cycle geometry at all singular points.

14.1. Test Case 1: 15-degree function expanded at the origin, $\mathcal{G} = 86$.

$$f_1(z, w) = (z^{30} + z^{32}) + (z^{14} + z^{20}) w^5 + (z^5 + z^9) w^9 + (z + z^3) w^{12} + 6w^{14} + (2 + z^2) w^{15} \quad (23)$$

Timing data is shown in Table 4. The base expansions are done to at least 1000 terms and the comparison series to at least 100 terms at 1000 digits of precision.

TABLE 4. Test Case 1 Timing Data

Singular points	Initial segments	Base gen. expansions	Comparison expansions	CT	IT
(179, 1.9 s)	8 s	(5, 13.4 m)	(125, 37.5 m)	1.3 m	2.7 m

Singular points: (Total points, time), **Initial segments:** time

Base expansion: (Total generators, time), **Comparison expansions:** (Total sing. pts., time)

CT: comparison test time, **IT:** Integration Test time

s: Seconds, **m:** Minutes **h:** hours

Table 5 summarizes the CLSP and accuracy results.

TABLE 5. Test Case 1 Summary Report at the origin

Type	CLSP	R	Terms	a	b	c	d	Var
F_5^{16}	27	0.641328	1987	3.19696	-0.329926	0.00567716	-0.433846	0.23481
F_4^9	7	0.504901	2022	3.4831	-0.219358	0.00355264	-0.434293	0.228403
F_3^4	2	0.166817	1017	3.42982	-0.287641	0.00466601	-0.434467	0.173804
V_2^1	2	0.166817	1024	3.5265	-0.224677	0.00418632	-0.434702	0.259237
T	118	1.09352	1024	2.83953	-0.287592	0.00193844	-0.434512	0.565284

Type: Branch type (see Appendix 16), **CLSP:** Convergence-limiting singular point,

R: Radius of convergence, **Terms:** Series length, **(a,b,c,d):** constants for $A(r_f, o)$, **Var:** Variance

The accuracy constants (a, b, c, d) can be used to determine the approximate order needed to achieve a desired accuracy. For example, if a value of the F_5^{16} branch at $z = 1/3Re^{3\pi i/4}$ to 20 digits of accuracy is desired, that is, $e_a = 20$, solve $O(1/3, 20)$ where

$$O(r_f, e_a) = \left\lceil \frac{a + 0.329926 \log(r) - 3.19696}{0.00567716 - 0.433846 \log(r)} \right\rceil.$$

This gives an order estimate of 35. A simple scan of the expansion exponents can determine the series term corresponding to an order of 35. This turns out to be term 99. The first 99 terms of the generator series at z leads to a value accurate to approximately 20 digits. In this case, the accuracy is 20 digits as shown by comparing the value to the corresponding root of $f_1(z, w) = 0$. The estimated accuracy however will often differ from the actual error by a small amount as shown by the variance in Table 5.

The constants (a, b, c, d) for each branch in Table 5 are similar in size. This means that a single average accuracy function could be generated for all the branches in this case. However in other cases, the accuracy constants can be quite different.

Table 6 summarizes the ramification profile describing the cycle geometry at all singular points. The set of singular points minimally-ramified is $\{\bar{s}_n\}$ with ramification $(2, [13, 1])$ signifying a single 2-cycle branch and 13 single-cycle branches. Singular points with higher ramifications are listed separately or $\{u_i\}_n$ for multiple singular points with the same ramification.

TABLE 6. Test Case 1 Ramification profile, $\mathcal{K} = 200$

Singular point	Cycles
s_1	$(1, 2, 3, 4, 5)$
s_{110}	$(9, [6, 1])$
s_{111}	$(9, [6, 1])$
$\{p_i\}_2$	$[15, 1]$
$\{\bar{s}\}_{174}$	$(2, [13, 1])$
s_∞	$[15, 1]$

$\{p_i\}_2$: set of two poles

[m,n]: n -cycle branches, m total

$\{\bar{s}\}_n$: remaining n singular points minimally ramified

14.2. Test Case 2: 4-degree function with polynomial solution at the origin, $\mathcal{G} = 0$.

$$f_2(z, w) = (1 - 3z + 3z^2 - 1z^3) + (-4 + 8z - 4z^2)w + (6 - 6z)w^2 + (-4)w^3 + (1)w^4 \quad (24)$$

This function has two singular points $\{0, 1\}$ and a 4-cycle polynomial solution at the origin:

$$\begin{aligned} w_1(z) &= 1 - z^{1/4} + z^{1/2} - z^{3/4} \\ w_2(z) &= 1 - iz^{1/4} - z^{1/2} + iz^{3/4} \\ w_3(z) &= 1 + z^{1/4} + z^{1/2} + z^{3/4} \\ w_4(z) &= 1 + iz^{1/4} - z^{1/2} - iz^{3/4}. \end{aligned} \quad (25)$$

In this case, the modular operation of the Newton iteration step (15) returns a finite polynomial after reaching the maximum zero modular value N_{zm} . And since the solutions are finite, $R = \infty$. However this can only be true if the function does not ramify or is non-polar at $z = 1$. That is, the singularity at $z = 1$ is removable. We can show this as follows:

The expansions at $z = 1$ are four 1-cycles with starting terms:

$$\begin{aligned} w_1(z) &= -0.5z + 0.0625z^2 - 0.03125z^3 + 0.0205078z^4 + \dots \\ w_2(z) &= (-0.5 - 0.5I)z + (0.125 + 0.I)z^2 - (0.0625 - 0.015625I)z^3 + \dots \\ w_3(z) &= (-0.5 + 0.5I)z + (0.125 + 0.I)z^2 - (0.0625 + 0.015625I)z^3 + \dots \\ w_4(z) &= 4 + 1.5z - 0.3125z^2 + 0.15625z^3 + \dots \end{aligned} \quad (26)$$

The solutions to $f_2(1, w) = 0$ are $\{0, 0, 0, 4\}$ and these are the values of (26) at $z = 0$ and note

$$\begin{aligned} \frac{dw}{dz} &= \lim_{(z,w) \rightarrow (1,0)} \left(-\frac{f_z(z, w)}{f_w(z, w)} \right) \rightarrow \frac{0}{0} \\ \frac{dw}{dz} &= \lim_{(z,w) \rightarrow (1,4)} \left(-\frac{f_z(z, w)}{f_w(z, w)} \right) = -\frac{3}{2}. \end{aligned} \quad (27)$$

However the derivatives of (26) at $z_r = 0$ are finite so that we can immediately solve for the indeterminate limits

$$\frac{dw}{dz} = \lim_{(z,w) \rightarrow (1,0)} \left(-\frac{f_z(z,w)}{f_w(z,w)} \right) = \{-0.5, -0.5 - 0.5i, -0.5 + 0.5i\}. \quad (28)$$

And since the function fully-ramifies at the origin, the four expansions at $z_a = 1$ all have $R = 1$. This is confirmed by the Root Test and both series comparison and integration tests. Accuracy results are given in Table 7. And by virtue of the singularity at the origin, the expansions at $z = 1$ all have radii of convergence of 1. Finally, as this branch is equivalent to the function $f(z) = z^{1/4}$, the ramification at infinity will also be 4-cycle and thus the genus is $(3+3)/2 + 1 - 4 = 0$. Timing for this case was minimal.

TABLE 7. Test Case 2 Summary Report at $s_2 = 1$

Type	CLSP	R	Terms	a	b	c	d	Var
1E	1	1.	1024	3.07174	-0.302067	0.00142759	-0.434367	0.156447
2E	1	1.	1024	2.83926	-0.321447	0.00161223	-0.434362	0.164684
3E	1	1.	1024	2.83926	-0.321447	0.00161223	-0.434362	0.164684
T	1	1.	1024	2.59935	-0.324381	0.00175722	-0.434358	0.195594

14.3. Test Case 3: 34-degree function expanded at s_{487} , $\mathcal{G} = 264$.

$$\begin{aligned} f_3(z, w) &= \left(-\frac{1043}{60} - \frac{5}{3}z^2 + 2z^3 - 4z^4 - \frac{6}{5}z^5 - \frac{2}{3}z^9 + \frac{8}{3}z^{14} + \frac{25}{4}z^{15} + 4z^{16} \right) \\ &\quad + \left(\frac{11}{3} \right) w^5 + \left(-\frac{8}{3} \right) w^{12} + \left(-\frac{38}{5} - \frac{1}{2}z \right) w^{34} \\ &= 0 \end{aligned} \quad (29)$$

This function was selected to stress-test the methods of finding CLSPs and also to study the fully-ramified branch at infinity. The function has 493 singular points with s_{487} ramifying into a 22-cycle and 12 single cycles and having 13 nearest neighbors with an average separation distance of 10^{-35} .

Root Tests results were not precise enough to distinguish individual singular points near the expansion center and returned 1.056×10^{-35} as the estimate for the single-cycle branches and 1.09×10^{-35} for the 22-cycle branch identifying s_{487} as the estimated CLSP of the base expansions. This in itself is not an error but rather attempting to use the Root Test at an extremely small tolerance. The comparison sequence however can be set to a reasonable number of singular points and in this case was set to the first 25 singular point in the singular sequence.

However, the comparison test failed to identify CLSPs at the default settings as the base series were not accurate enough to meet the comparison tolerances of 10^{-6} . The Integration Test likewise failed to identify CLSPs with a working precision of 40 and default integration method. However, increasing the integration working precision of the integration test from 40 to 80 with “StiffnessSwitching” method met the tolerances and found all CLSPs in 11.5 minutes. These results are shown in Table 9.

TABLE 8. Test Case 3 Timing Data

Singular points	Initial segments	Base expansion	Comparison expansions	CT	IT
(493, 54s)	(50s)	(13, 13.2m)	(25, 7.5mh)	-	11.5 m

The function has a fully-ramified 34-cycle branch at infinity which means the CLSP is s_2 relative to infinity. The default setting for the comparison test were not sufficient to identify this CLSP. The integration test using default integration methods also failed but succeeded in identifying s_2 as the CLSP using Mathematica’s `NDSolve StiffnessSwitching` method.

TABLE 9. Test Case 3 Summary Report at s_{487}

Type	CLSP	R	Terms	a	b	c	d	Var
1T	493	1.0511×10^{-35}	1024	2.57488	-0.408571	0.00198314	-0.434325	0.246471
2T	488	1.0511×10^{-35}	1024	2.43652	-0.456495	0.00189591	-0.434416	0.221283
3T	489	1.0511×10^{-35}	1024	2.42991	-0.493089	0.00181696	-0.434467	0.24568
4T	485	1.0511×10^{-35}	1024	2.58246	-0.391823	0.00188475	-0.434426	0.304147
5T	486	1.0511×10^{-35}	1024	2.49944	-0.447571	0.00205355	-0.434356	0.244369
6T	482	1.0511×10^{-35}	1024	2.60673	-0.384546	0.0019365	-0.434366	0.241232
7T	481	1.0511×10^{-35}	1024	2.52156	-0.458827	0.00198745	-0.434316	0.238367
8T	484	1.0511×10^{-35}	1024	2.64395	-0.365494	0.00186476	-0.434422	0.242922
9T	483	1.0511×10^{-35}	1024	2.61553	-0.379034	0.00196351	-0.434371	0.247183
10T	491	1.0511×10^{-35}	1024	2.66054	-0.378256	0.00185278	-0.434409	0.229304
11T	490	1.0511×10^{-35}	1024	2.56919	-0.427104	0.00188795	-0.434372	0.248727
12T	492	1.0511×10^{-35}	1024	2.60019	-0.386299	0.00190533	-0.434368	0.246803
P_{22}^{-1}	492	1.0511×10^{-35}	2021	1.64383	-0.210138	0.0150419	-0.433515	0.183742

Actual values of R differ from the 1.0511×10^{-35} value given for brevity
For precise values of R use $R = |s_{487} - s_{CLSP}|$

TABLE 10. Test Case 3 Ramification profile, $\mathcal{K} = 594$

Singular point	Cycles
$\{u_i\}_{16}$	$(5, [29, 1])$
s_{487}	$(22, [12, 1])$
$\{\bar{s}\}_{476}$	$(2, [32, 1])$
s_∞	(34)

$$\{u_i\}_n = \{51, 52, 57, 58, 134, 177, 178, 255, 256, 281, 282, 357, 358, 426, 427, 440\}$$

14.4. Test Case 4: 35-degree function expanded at infinity, $\mathcal{G} = 32$.

$$\begin{aligned}
f_4(z, w) = & \left(-\frac{31}{10} + \frac{179}{30}z + \frac{1}{4}z^2\right) + \left(-\frac{7}{4}\right)w^2 + (4)w^3 + \left(-\frac{1}{2} - \frac{5}{2}z\right)w^8 + \left(\frac{11}{3}\right)w^{10} + \left(6 + \frac{5}{2}z\right)w^{14} \\
& + (5)w^{18} + \left(-\frac{64}{15}\right)w^{20} + \left(\frac{11}{2} - \frac{1}{2}z^2\right)w^{22} + \left(-\frac{9}{2} + \frac{7}{3}z\right)w^{25} + \left(\frac{18}{5} - \frac{3}{4}z^2\right)w^{28} \\
& + \left(-\frac{3}{2} - 1z\right)w^{33} + \left(-\frac{8}{3}\right)w^{35} \\
& = 0
\end{aligned} \tag{30}$$

First consider $f_4(z, w)$ which has 127 finite singular points all of which are minimally-ramified. In order to obtain the ramification at infinity, $f_4(z, w)$ is transformed to $g_4(z, w) = z^\delta f_4\left(\frac{1}{z}, w\right)$ with δ the largest

power of z in $f_4(z, w)$. In this case $\delta = 2$ giving:

$$\begin{aligned}
g_4(z, w) &= \left(\frac{1}{4} + \frac{179}{30}z - \frac{31}{10}z^2\right) + \left(-\frac{7}{4}z^2\right)w^2 + (4z^2)w^3 + \left(-\frac{5}{2}z - \frac{1}{2}z^2\right)w^8 + \left(\frac{11}{3}z^2\right)w^{10} \\
&= + \left(\frac{5}{2}z + 6z^2\right)w^{14} + (5z^2)w^{18} + \left(-\frac{64}{15}z^2\right)w^{20} + \left(-\frac{1}{2} + \frac{11}{2}z^2\right)w^{22} \\
&+ \left(\frac{7}{3}z - \frac{9}{2}z^2\right)w^{25} + \left(-\frac{3}{4} + \frac{18}{5}z^2\right)w^{28} + \left(-z - \frac{3}{2}z^2\right)w^{33} + \left(-\frac{8}{3}z^2\right)w^{35} \\
&= 0.
\end{aligned} \tag{31}$$

Then an expansion of $w(z)$ at $z_a = 0$ through $g_4(z, w)$ is the expansion of $w(z)$ defined by $f_4(z, w)$ at infinity. The base series and comparison series were next computed relative to $g_4(z, w)$. Table 11 is the timing summary.

TABLE 11. Test Case 4 Timing Data at infinity

Singular points	Initial segments	Base expansion	Comparison expansions	CT	IT
(128,2 s)	(15 s)	(30,3.4 h)	(32,68 m)	2.6 m	7.4 m

The expansion at infinity ramified as $(5, 2, [28, 1])$. Table 12 is a Summary Report. Consider the 5-cycle branch expansions of P_5^{-1} of $g_4(z, w)$ with $R = 0.04874$. These are expansions of $w(z)$ centered at infinity which means the five values of $w(z)$ associated with this branch at $z_a = \frac{1}{z_r}$ are the same five branch values $\{v_s\}$ at z_r . For example, let $z_a = 200 + 100i$ which is outside the domain of finite singular points of f_4 and therefore $z_r = \frac{1}{200 + 100i} = 0.004 - 0.002i$ is closer to infinity than the nearest singular point of f_4 . Then the P_5^{-1} expansions will converge at z_r . The 35 values of $w(z_a)$ are easily found by solving for the roots $\{w_i\} = f_4(z_a, w) = 0$. Among these roots are the five values of P_5^{-1} at z_r :

$$-2.83979 - 0.469744i, -1.3576 + 2.63902i, -0.501188 - 2.89321i, 2.05904 + 2.02105i, 2.62398 - 1.28185i.$$

The following are the roots $\{w_i\}$ with the above branch values highlighted in red.

$$\begin{aligned}
&-3.92407 + 9.53357i, \textcolor{red}{-2.83979 - 0.469744i}, \textcolor{red}{-1.3576 + 2.63902i}, -0.940335 + 0.00182458i, -0.922871 + 0.235934i, \\
&-0.922161 - 0.232486i, -0.888861 - 0.448904i, -0.886022 + 0.452484i, -0.783866 - 0.586343i, -0.780327 + 0.586443i, \\
&-0.604223 - 0.72708i, -0.601147 + 0.730563i, \textcolor{red}{-0.501188 - 2.89321i}, -0.403707 - 0.850957i, -0.399549 + 0.853659i, \\
&-0.187928 - 0.945784i, -0.181958 + 0.946171i, -0.000537808 - 0.999928i, -0.000128033 + 1.00055i, 0.182496 - 0.945415i, \\
&0.187148 + 0.94525i, 0.399708 - 0.85302i, 0.403067 + 0.850813i, 0.601121 - 0.730076i, 0.603749 + 0.727117i, \\
&0.781083 - 0.585674i, 0.783141 + 0.585525i, 0.887975 - 0.453228i, 0.889622 + 0.446953i, 0.92263 + 0.231865i, \\
&0.923506 - 0.236407i, 0.940601 - 0.00209421i, \textcolor{red}{2.05904 + 2.02105i}, \textcolor{red}{2.62398 - 1.28185i}, 3.9374 - 9.5466i
\end{aligned}$$

Another way to visualize the expansions at infinity is to consider the ramification of $f_4(z, w)$ outside a disc containing all the finite singular points, that is a disc $r < |s_{127}| \approx 27.15$. This ramification is the same $(5, 2, [28, 1])$ ramification as that at infinity and is in fact the same set of branches. That is, we can compute the ramification at infinity for $f_4(z, w)$ by simply computing the ramification of $f_4(z, w)$ at say $r = 28$. See [On the branching geometry of algebraic functions](#) for a method of doing this.

TABLE 12. Test Case 4 summary report at the point of infinity, i.e., g_4 expanded at $z = 0$

Type	CLSP	R	Terms	a	b	c	d	Var
1T	23	0.0416879	1024	3.28983	-0.360237	0.00187946	-0.434348	0.186178
2T	2	0.0368337	1024	3.45719	-0.343809	0.00191956	-0.434455	0.25136
3T	3	0.0368337	1024	3.40354	-0.405533	0.0019289	-0.434433	0.257028
4T	2	0.0368337	1024	3.34071	-0.453646	0.00192991	-0.434402	0.289739
5T	3	0.0368337	1024	3.27402	-0.498051	0.00198714	-0.434375	0.335869
6T	5	0.0369532	1024	3.67988	-0.426256	0.00192521	-0.43436	0.253784
7T	4	0.0369532	1024	3.70872	-0.420795	0.00196974	-0.434302	0.250291
8T	24	0.0419264	1024	3.26493	-0.392033	0.001903	-0.434354	0.220053
9T	25	0.0419264	1024	3.44163	-0.341589	0.00175748	-0.434415	0.21876
10T	13	0.0401948	1024	3.22901	-0.429983	0.00206575	-0.434317	0.270064
11T	12	0.0401948	1024	3.16109	-0.464687	0.00199673	-0.43438	0.303588
12T	13	0.0401948	1024	3.17537	-0.444561	0.00193504	-0.434374	0.239211
13T	12	0.0401948	1024	3.34242	-0.380652	0.00192249	-0.43438	0.221718
14T	28	0.0590922	1024	3.85445	-0.402529	0.00188963	-0.434352	0.247296
15T	29	0.0590922	1024	3.82279	-0.484877	0.00188897	-0.434324	0.247753
16T	10	0.0391605	1024	3.3216	-0.409763	0.00199395	-0.434323	0.220968
17T	11	0.0391605	1024	3.32488	-0.391127	0.00195106	-0.434362	0.228586
18T	10	0.0391605	1024	3.24861	-0.444286	0.00197163	-0.434382	0.270096
19T	11	0.0391605	1024	3.265	-0.437944	0.00201653	-0.434335	0.270439
20T	16	0.0408681	1024	3.33897	-0.353798	0.00190399	-0.434374	0.202345
21T	15	0.0408681	1024	3.28935	-0.354593	0.00189579	-0.43441	0.207717
22T	8	0.0383842	1024	3.83458	-0.418136	0.00191619	-0.434332	0.237896
23T	9	0.0383842	1024	3.93489	-0.370628	0.00194949	-0.434367	0.218989
24T	7	0.0378856	1024	3.36544	-0.388662	0.0019894	-0.434436	0.264613
25T	6	0.0378856	1024	3.35258	-0.425374	0.00204086	-0.434361	0.309241
26T	7	0.0378856	1024	3.3512	-0.423055	0.00192371	-0.434414	0.251619
27T	6	0.0378856	1024	3.43569	-0.376695	0.00187883	-0.434427	0.252273
28T	26	0.0427618	1024	3.29122	-0.404697	0.00182958	-0.434401	0.215776
P_5^{-1}	27	0.0487394	1020	3.27798	-0.0326398	0.0077994	-0.434404	0.111103
P_2^{-1}	27	0.0487394	1023	2.81247	-0.33028	0.0036736	-0.434123	0.207571

TABLE 13. Test Case 4 ramification profile, $\mathcal{K} = 132$

Singular point	Cycles
$\{\bar{s}\}_{127}$	$(2, [33, 1])$
s_∞	$(5, 2, [28, 1])$

14.5. **Test Case 5: 50-degree function expanded at the origin, $\mathfrak{G} = 2268$.**

$$\begin{aligned}
f_5(z, w) = & \left(2z^6 + \frac{1}{2}z^7 - \frac{5}{4}z^{11} + 4z^{22} + \frac{29}{10}z^{34} - 1z^{40} - \frac{13}{2}z^{43}\right) + \left(\frac{3}{5}z^{10} + \frac{7}{4}z^{24} - \frac{1}{4}z^{50}\right)w^2 \\
& + \left(2z^{17} + \frac{7}{2}z^{34}\right)w^3 + \left(-\frac{3}{2}z^{30} + \frac{4}{3}z^{38} + \frac{8}{5}z^{42}\right)w^4 + \left(-\frac{6}{5}z^2 - \frac{1}{2}z^6 + \frac{7}{3}z^{31}\right)w^9 \\
& + \left(-\frac{2}{5}z^{11} - \frac{3}{2}z^{26} + 1z^{45}\right)w^{10} + \left(\frac{7}{5}z^{24} - 6z^{32} - 6z^{49}\right)w^{14} \\
& + \left(-\frac{3}{4}z^5 + \frac{7}{3}z^{21} - \frac{1}{4}z^{26} + \frac{4}{5}z^{27} + \frac{4}{3}z^{32} - 2z^{36} + \frac{1}{3}z^{39} - \frac{3}{4}z^{41} - z^{43}\right)w^{16} \\
& + (-6z^{14} - 2z^{31} - z^{33})w^{18} + \left(-2z^{27} - \frac{8}{3}z^{50}\right)w^{22} + \left(4z^8 + \frac{4}{5}z^{25} - \frac{3}{2}z^{27}\right)w^{24} \\
& + \left(-3z^4 + \frac{8}{3}z^{22} - \frac{8}{5}z^{43}\right)w^{33} + \left(\frac{7}{3}z^{14} - \frac{3}{2}z^{18}\right)w^{34} + \left(-4 + 8z^{13} - \frac{7}{4}z^{47}\right)w^{36} \\
& + \left(z^2 - \frac{1}{4}z^7\right)w^{38} + \left(-\frac{1}{2}z^{20} - z^{29} + z^{46}\right)w^{40} + \left(\frac{1}{3}z^{10} + \frac{7}{4}z^{11} + \frac{8}{5}z^{21}\right)w^{47} \\
& + \left(\frac{2}{3}z^2 + 6z^{26} + \frac{3}{5}z^{43}\right)w^{48} + \left(-z^9 + \frac{1}{4}z^{13} + 2z^{14} + 2z^{18} + z^{36} - 2z^{44}\right)w^{49} \\
& + \left(-\frac{1}{3}z^{23} - \frac{7}{2}z^{40} + z^{42}\right)w^{50} \\
& = 0
\end{aligned} \tag{32}$$

This function has 4584 singular points. The singular point at the origin was selected as s_b and the Root Test indicated a comparison sequence of s_2 through s_{100} . Table 14 is the timing data, and Table 15, the Summary Report.

TABLE 14. Test Case 5 Timing Data

Singular points	Initial segments	Base expansion	Comparison expansions	CT	IT
(4584,3.76 h)	(4584,49 m)	(6,50 m)	(100,11 h)	1.3 m	2.7 m

TABLE 15. Test Case 5 Summary Report at the origin

Type	CLSP	R	Terms	a	b	c	d	Var
V_9^4	2	0.564982	1969	3.32621	-0.245552	0.00915745	-0.433441	0.165712
V_{27}^2	2	0.564982	1837	2.88746	-0.0586786	0.0251435	-0.435114	0.163804
$1 P_6^{-1}$	98	0.791246	2004	2.60055	-0.314091	0.00555285	-0.433077	0.200407
$2 P_6^{-1}$	94	0.786365	2004	2.47551	-0.340257	0.0073696	-0.432927	0.215718
L_{-7}	92	0.75919	1020	0.865693	-0.405906	0.00141605	-0.43457	0.285315
L_{-14}	92	0.75919	1017	0.694339	-0.323955	0.00148271	-0.434907	0.191351

TABLE 16. Test Case 5 Ramification profile, $\mathcal{K} = 4634$

Singular point	Cycles
s_1	$(9, 27, [2, 6], [2, 1])$
$\{p_i\}_{19}$	$[50, 1]$
$\{\bar{s}\}_{4564}$	$(2, [48, 1])$
s_∞	$(14, 13, 2, [21, 1])$

$$\{p_i\}_{19} = \{1, 229, 230, 233, 234, 238, 239, 248, 249, 262, 263, 276, 277, 300, 301, 324, 325, 334, 4537, 4538\}$$

14.6. Test Case 6: 25 degree function with complex coefficients expanded at s_{29} , $\mathfrak{g} = 326$.

$$\begin{aligned}
f_6(z, w) = & -\left(\frac{311}{20}i + \frac{467}{30}\right) - \left(\frac{16}{3}i + \frac{3}{2}\right)z + \left(\frac{1}{4} - \frac{3}{4}i\right)z^3 + \left(\frac{9}{4}i + 3\right)z^4 - \left(\frac{3}{10} - \frac{21}{5}i\right)z^5 \\
& - \left(1 - \frac{7}{3}i\right)z^7 - \frac{5}{3}z^8 - \left(\frac{12}{5}i + 1\right)z^9 - \left(2i + \frac{5}{4}\right)z^{11} - \left(\frac{1}{4} - 3i\right)z^{12} \\
& - \left(\frac{27}{5}i + 3\right)z^{13} + \left(\frac{19}{6}i + 7\right)z^{14} + (3i - 2)z^{15} \\
& + \left(-\left(\frac{59}{60}i + \frac{13}{10}\right) + (1 - 3i)z^{12} + \left(4i + \frac{4}{5}\right)z^{13}\right)w \\
& + \left(-\left(\frac{71}{10} - \frac{1}{6}i\right) - \left(\frac{8}{3} - 6i\right)z^2 + (-i - 8)z^8\right)w^6 \\
& + \left(\frac{15}{2}i + \frac{116}{15}\right)w^8 + \left(\left(\frac{12}{5} - \frac{15}{4}i\right) + \frac{2iz^3}{5} + \left(-7i - \frac{5}{2}\right)z^{10}\right)w^9 \\
& + \left(\frac{13}{2} - \frac{32}{5}i\right)w^{10} \\
& + \left(-\left(\frac{19}{4}i + \frac{5}{3}\right) - \left(3 - \frac{6}{5}i\right)z^3 + \left(\frac{3}{2}i - \frac{3}{4}\right)z^{13}\right)w^{13} \\
& + \left(\left(\frac{47}{15}i + \frac{155}{12}\right) - \left(\frac{1}{6} - \frac{1}{2}i\right)z^2 - \left(\frac{1}{5} - \frac{5}{3}i\right)z^{10} + \left(\frac{3}{2}i - 2\right)z^{14}\right)w^{14} \\
& + \left(-\left(\frac{109}{12} - \frac{37}{12}i\right) - \frac{iz^5}{2}\right)w^{18} \\
& + \left(\left(5i + \frac{6}{5}\right) - \left(\frac{1}{5}i + \frac{7}{4}\right)z^{12} + \left(\frac{8}{5}i + 7\right)z^{14}\right)w^{21} \\
& + \left(\left(\frac{2}{5} - \frac{13}{10}i\right) - \frac{8}{3}z^7 + (-2i - 1)z^{10}\right)w^{25}
\end{aligned} \tag{33}$$

This function has 660 finite singular points and was expanded at pole s_{29} . Table 17 gives the timing data and Tables 18 and 19 detail the accuracy and ramification data.

TABLE 17. Test Case 6 Timing Data at s_{29}

Singular points	Initial segments	Base gen. expansions	Comparison expansions	CT	IT
(660, 30 m)	(660, 3.3 m)	(22, 2 h)	(27, 29 m)	1.3 m	3.4 m

TABLE 18. Test Case 6 Summary Report at s_{29}

Type	CLSP	R	Terms	a	b	c	d	Var
1T	38	0.0167133	1024	3.17032	-0.41029	0.00192871	-0.434412	0.219225
2T	56	0.0982504	1024	3.69649	-0.368397	0.00189034	-0.434359	0.242937
3T	177	0.173224	1024	3.68729	-0.446054	0.00194646	-0.434356	0.248846
4T	354	0.208561	1024	3.54559	-0.371434	0.00189941	-0.434436	0.254165
5T	10	0.197401	1024	3.98117	-0.433098	0.0018211	-0.434431	0.215548
6T	232	0.156337	1024	3.64785	-0.336867	0.00194168	-0.434384	0.227871
7T	108	0.149061	1024	3.68843	-0.385887	0.00197982	-0.434356	0.249595
8T	41	0.0672525	1024	3.48234	-0.389387	0.00182101	-0.434454	0.241994
9T	125	0.101533	1024	3.82856	-0.431569	0.00196967	-0.434425	0.258889
10T	13	0.0970926	1024	3.53643	-0.479354	0.00191281	-0.43444	0.25699
11T	125	0.101533	1024	3.90238	-0.37848	0.00192665	-0.434415	0.25622
12T	264	0.16936	1024	3.74861	-0.428541	0.00204153	-0.434296	0.243689
13T	20	0.0362971	1024	3.44335	-0.374599	0.0018982	-0.434408	0.245484
14T	129	0.109811	1024	3.58688	-0.357851	0.00184152	-0.434469	0.225132
15T	195	0.140624	1024	3.62277	-0.324291	0.00190887	-0.434374	0.228172
16T	86	0.138713	1024	3.56908	-0.453317	0.00192339	-0.434365	0.252658
17T	210	0.142419	1024	3.74149	-0.386165	0.00196671	-0.43432	0.233369
18T	181	0.201697	1024	3.64415	-0.423745	0.00191286	-0.43442	0.276286
19T	120	0.16032	1024	3.32947	-0.453331	0.0020065	-0.434385	0.269883
20T	173	0.175719	1024	3.62089	-0.440735	0.00191062	-0.434385	0.24661
21T	35	0.0170704	1024	3.26908	-0.40917	0.00189352	-0.434389	0.238545
P_4^{-1}	38	0.0167133	1021	3.08615	-0.0848102	0.00655571	-0.434368	0.160934

In this case $R = |s_{29} - s_{CLSP}|$

TABLE 19. Test Case 6 Ramification profile, $\mathcal{K} = 700$

Singular point	Cycles
$\{p_i\}_{10}$	$(4, [21, 1])$
$\{\bar{s}\}_{650}$	$(2, [23, 1])$
s_∞	$(21, [4, 1])$

$$\{p_i\} = \{29, 30, 37, 43, 76, 88, 212, 316, 486, 509\}$$

15. CONCLUSIONS

- (1) A numerical approach to Newton polygon initially seems problematic. However this work includes several error checking algorithms:
 - (a) **Cycle check-sum:** The sum of the conjugate classes at any expansion center must equal to the degree of the function in w ,
 - (b) **Global cycle check-sum:** The Riemann-Hurwitz sum must be a positive number,
 - (c) **Removal of coefficient zeros:** In order to minimize residual errors, coefficient zeros are removed from f and its iterates before processing by the Newton polygon algorithm,
 - (d) **Precision monitoring:** The precision of the calculations are monitored throughout the algorithms and terminate the analysis if it drops below 900 digits,
 - (e) **Accuracy results:** The accuracy results of a set of expansions would not follow the log-linear trend with low variance if a branch was incorrectly computed.

These measures reduce the potential of errors. However, there exists functions which can usurp this numeric approach. These would include the following scenarios:

- (a) **Singular size limits:** Functions with very small singular sizes coupled with very large exponents sufficient to compromise a realistic level of precision achievable in a reasonable amount of time,

- (b) **High polygon iterates:** Functions which entail multiple polygon iterations sufficient to reduce the precision of the characteristic equations below a reasonable level of numeric precision,
 - (c) **High polygon iterates:** It is likely there are functions with arbitrary polygon iterates which would decrease the precision of the calculations beyond any effort to keep the results above a minimum level,
 - (d) **High poly mod function:** Functions with extremely large gaps between successive expansion terms would cause the modular operation of (15) to exceed the (arbitrary) maximum number of zero term iterations. In this case, an infinite power expansion would be identified as a fractional polynomial.
- (2) Identifying conjugate classes and only expanding generator series of each class is an improvement to the standard approach to expanding all initial segments of a Newton Polygon expansion. The greatest time saving is when the conjugate set at an expansion center is highly ramified. An example of this is the 50-degree function of test case 4 which only required iterating six generator series in 50 minutes rather than an estimated seven hours to generate the full 50 set.
 - (3) The test cases were designed to stress-test the series comparison and integration tests with complex functions. With minor tuning of the methods, CLSPs and corresponding radii of convergence results agreed well with the estimated values determined by the Root Test when the separation tolerance was set to 1/10 the separation distance of the branch values. In cases where the comparison test and integration test succeeded in identifying CLSPs, both identified the same CLSP for each branch. In Test Case 3 where the comparison test failed, this was due to extremely small singular perimeters on the order of 10^{-35} causing the base expansions to be evaluated extremely close to their radii of convergence. However the integration test succeeded with proper adjustments to the integration method.
 - (4) The accuracy and order functions were found to agree well with the actual accuracies of the series as shown by the accompanying low variances of the fit function showing $A(r_f, o)$ to be a robust predictor of accuracy in the testing range.
 - (5) The close approximation of the Root Test to the CLSPs shows the Root Test to be a reliable means of estimating radii of convergences.
 - (6) This work opens the subject to further research:
 - (a) Find and analyze function which entail more polygon iterations,
 - (b) Find and analyze functions with fractional polynomial solutions,
 - (c) Further fine-tuning the algorithm as problem cases arise,
 - (d) Reducing execution time,
 - (e) Identifying problem functions and updating the method to accommodate them.

16.

Appendix A: Branch types used in this paper

In the following branch descriptors, all exponents $\frac{q}{p}$ of a series are presumed placed under a least common denominator p .

Type T: Power series with positive integer powers (Taylor series). These are 1-cycle branches.

Type E: 1-cycle T branch with a removable singular point at its center.

Type F_p^q : p -cycle branch with $p > 1$ of order q with non-negative exponents and lowest non-zero exponent $\frac{q}{p}$ with $q > p$. These branches are multi-valued consisting of p single-valued sheets with a finite tangent at the singular point. An example F_2^3 series is $z^{3/2} + z^2 + \dots$.

Type V_p^q : p -cycle branch with $p > 1$ of order q with non-negative exponents and lowest non-zero exponent $\frac{q}{p}$ with $q < p$ and vertical tangent at center of expansion. An example V_4^3 series is $z^{3/4} + z^2 + \dots$.

Type P_p^q : p -cycle branch unbounded at center with $p > 1$ of order q having negative exponents with lowest negative exponent $\frac{q}{p}$. An example 3-cycle P series of order -1 is $z^{-1/3} + z^2 + \dots$. An example 3-cycle P series of order -5 is $z^{-5/3} + z^{-1/3} + \dots$.

Type L^q : Branch with Laurent series of order q as the Puiseux series. An example L^{-2} series is $1/z^2 + 1/z + z^2 + \dots$.

REFERENCES

- [1] Bliss, Gilbert A. *Algebraic Functions*. New York: Dover Publications, Inc., 2004.
- [2] Brown, James and Ruel Churchill. *Complex Variables and Applications*. New York: McGraw Hill, 2004
- [3] Chudnovsky, D.V. and G.V. Chudnovsky. "On Expansion of Algebraic Functions in Power and Puiseux Series". *Journal of Complexity* **2**, 271-294 (1986).
- [4] Kung, H.T. and J. Traub, "All Algebraic Functions can be Computed Fast". *J. Assoc. Comput. Mach.* **25**, 245-260.
- [5] Markushevich, A.I., 1967. *Theory of Functions of a Complex Variable. Vol. III*. PrenticeHall, Englewood Cliffs, N. J.
- [6] Marsden, Jerrold and Michael Hoffman. *Basic Complex Analysis*. New York: W.H Freeman and Company, 1999.
- [7] Milioto, Dominic C. (2018, Dec. 8). Algebraic Functions, Retrieved from [Algebraic Functions and Iterated Exponentials](#).
- [8] Milioto, Dominic C. (2018, Jan. 13). On the branching geometry of algebraic functions, Retrieved from [On the branching geometry of algebraic functions](#)
- [9] Milioto, Dominic C. (2021, Dec. 13). Determining radii of convergence of fractional power expansions around singular points of algebraic functions, Retrieved from [Determining radii of convergence of fractional power expansions around singular points of algebraic functions](#)
- [10] Nowak, Krzysztof. *Some Elementary Proofs of Puiseux's Theorem*. Universitatis Iagellonicae ACTA Mathematica, Fasciculus XXXVIII, 2000.
- [11] Walker, Robert J. *Algebraic Curves*. Princeton: Princeton University Press, 1956.
- [12] Willis, Nicholas J., Didier, Annie K., Sonnanburg, Kevin M. *How to Compute a Puiseux Expansion*, arXiv: 0807.4674.1 [math.AG] 29 July, 2008

Email address: icorone@hotmail.com